

Enhanced Visualization of Detected 3D Geometric Differences

Gianpaolo Palma¹, Manuele Sabbadin^{1,2}, Massimiliano Corsini¹ and Paolo Cignoni¹

¹ Visual Computing Lab - ISTI - CNR, Pisa, Italy

² Department of Computer Science - University of Pisa, Pisa, Italy

Abstract

The wide availability of 3D acquisition devices makes viable their use for shape monitoring. The current techniques for the analysis of time-varying data can efficiently detect actual significant geometric changes and rule out differences due to irrelevant variations (like sampling, lighting, coverage). On the other hand, the effective visualization of such detected changes can be challenging when we want to show at the same time the original appearance of the 3D model. In this paper, we propose a dynamic technique for the effective visualization of detected differences between two 3D scenes. The presented approach, while retaining the original appearance, allows the user to switch between the two models in a way that enhances the geometric differences that have been detected as significant. Additionally, the same technique is able to visually hide the other negligible, yet visible, variations. The main idea is to use two distinct screen space time-based interpolation functions for the significant 3D differences and for the small variations to hide. We have validated the proposed approach in a user study on a different class of datasets, proving the objective and subjective effectiveness of the method.

Categories and Subject Descriptors (according to ACM CCS): I.4.8 [Image processing and Computer Vision]: Scene Analysis—Time-varying imagery I.3.7 [Computer Graphics]: Three-Dimensional Graphics and Realism—Animation

1. Introduction

The wide availability of acquisition devices like cameras, smartphones and low-cost portable 3D scanners (e.g. Google Tango, iSense, StructureSensor), makes today possible an easy and fast harvesting of 2D and 3D temporal data of the world around us. The correct temporal analysis and interpretation of this data are important for the automatic and robust detection of geometric changes in the scene and their following effective visualization. An enhanced and interactive visualization of temporal data that improves the perception and understanding of the changes in the scene is useful for several monitoring applications, like the environmental disaster prevention and management, the monitoring of construction sites, archeological excavations or urban environment, the preservation and presentation of Cultural Heritage artifacts in the time. In the last years several solutions have been proposed to solve the geometric change detection problem for different scenarios (3D reconstruction [YSL*14], urban growth analysis [TBP13] and natural events management [LFM*13]) using different input data (image datasets [PM07], 3D models and photos [TBP13], only 3D models [PCBS16]). On the other side, the effective visualization of temporal data was concentrated on time-varying volumetric data [WWS03] [KBH*10] [CRY11] and on videos [BDG15]. Usually, the existing solutions are based on static visualization of a single picture where the changes are encoded in some attribute like the color [PP95], the color saturation [WYM08], the surface bump [CRY11]. Sometimes, glyphs are employed for the same pur-

pose [TRM*01, CRY11]. The main problem of these solutions is that, by overlaying information or changing the original appearance of the presented objects, they can make difficult the understanding of the underlying shape. The typical example is the overlay of a color map that encodes the change and no-change areas with different colors, making harder the interpretation of the geometric and color information owned by the model (Figure 12). Additionally, the existing methods present a limited or completely absent user interaction allowing for example only the navigation of the volumetric data. Up to now, no methods are proposed to interact with the temporal dimension of the visual input in this specific context. For these reasons, we propose a real-time technique to improve the visualization of the detected geometric changes between two colored triangular meshes (Figure 1).

Given in input two 3D models of the same environment acquired at different times by 3D scanning or by multi-view image reconstruction our goal is to provide an interactive real-time visualization tool with three main features: a linear interaction model (slider) that allows to the user to continuously switch between the two time steps; to make clear and understandable what is changing in the scene; to preserve the original color and geometry attributes of the input models. In particular, we assume input 3D models with a change probability map computed in a preprocessing step which segments out the change and no-change areas. Our approach is based on the definition of a temporal interpolation between the 3D models that simultaneously tries to maximize the perception and

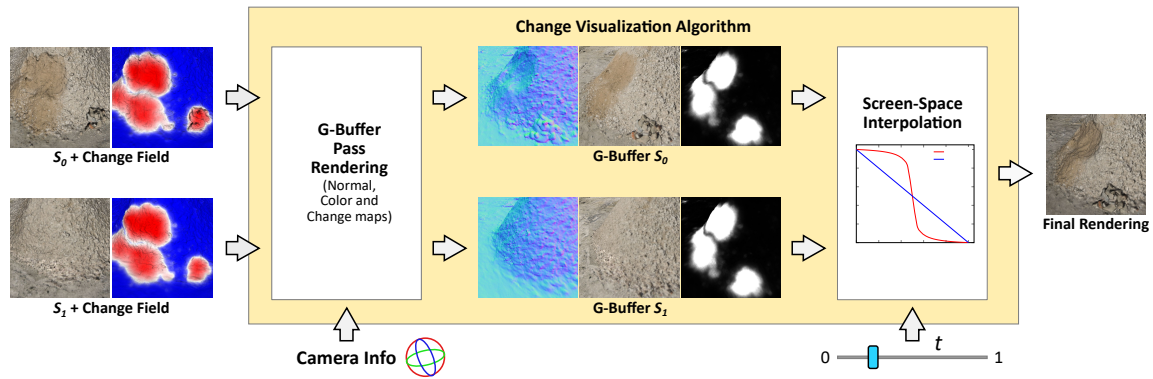


Figure 1: Algorithm overview. Starting from the input meshes S_0 and S_1 and the relative change field, the proposed real-time change visualization technique computes the geometry buffers for the two meshes and blends them in screen space using the time t with two different interpolation functions: $f_{\mathcal{C}}$ for the change pixels and $f_{\mathcal{NC}}$ for the no-change pixels, enhancing significant changes and hiding non-relevant, yet visible, differences.

the understanding of the most important and wide changed areas and to hide the non-significant, yet visible, differences that can distract the user's attention. These subtle differences are due to several reasons: geometric imperfections or noise due to the acquisition process, color differences due to different illumination conditions during the photographic acquisition (for what concern models coming from image-based reconstruction), changes at small scale.

The basic idea is to provide a screen-space interpolation technique of two renderings of the 3D models according to the user temporal interaction using different interpolation curves for the two classes of regions. For the choice of the interpolation curves we take into account the insights of the cognitive research on the Change Blindness phenomenon [SL97], that is the failure of the people to detect large changes in the scene, which normally would be easy to note, during the visual transition from one time to the next (see the video in the Additional Material for an example). Researchers have developed several different explanations for the occurrence of these phenomena [Sim00], especially when a visual disruption, like an eye movement, a flashed blank screen, a blink or a cut in a motion picture, is introduced during the transition between the two images. Interesting user test results were presented in Simons et al. [SFR00], where observers viewed a scene throughout the change and actively tried to find what was changing. In these experiments, the scene was viewed with a gradual condition, where the changes were presented as a 12 second fading of one image into the other, or with a disruption condition, created by an instantaneous transition between the images separated by a short blank gray screen (250ms). Two different types of changes were tested independently: objects that appear or disappear from the scene replaced by an appropriate scene background; objects or regions of the scene with a color change. The results coming from these experiments shows two important trends. When changes are sufficiently gradual, the visible change does not seem to draw attention, and large changes can go undetected. Furthermore, the color changes are detected less often than an addition/deletion change and their detection was better in the disruption condition than in the gradual condition. These results suggest us to use different screen-space interpolation curves for the change/no-change regions.

To summarize, the main contributions of this work are:

- A real-time visualization method that highlights the main temporal geometric changes and, at the same time, minimizes the perception of minor color and geometry inconsistencies using different temporal interpolation curves.
- A method that preserves, during the visual examination, all the color and geometric attributes of the input models without the use of overlay visual information, like an additional change color maps for example, that can make difficult the understanding of the color/geometric features of the underlying 3D models.
- A user study to assess the objective and subjective effectiveness of the proposed technique in the visualization of the temporal evolution of a changing scene.

A strength of the proposed method is the simple implementation and the negligible impact on the rendering time making easy its integration in any rendering system. For this purpose, we released this visualization tool as a web application available online.

2. Related Work

The comparative visualization of the temporal data was studied in several application fields, but up-to-now the attention was focused mainly on volumetric data. Pagendarm et al. [PP95] show the benefit of the scientific visualization using an overlay layer with color coding to compare flow simulation and experimental data. Gleicher et al. [GAW*11] present a survey of visual comparison techniques trying to extract a taxonomy with three categories: juxtaposition to present each object separately; superposition to present multiple objects in the same coordinate system; explicit encoding of the relationships related to visual connections between objects.

Several works have been developed for the medical and biological visualization. DeLeeuw et al. [LLV*00] present a system to visualize time-dependent data captured by a confocal microscopy of live 3D cells taking advantage of animations to improve the understating of some biological processes. Loomis et al. [LLD*97] propose a system for growing plant visualization based on a linear interpolation of different images acquired at different times.

Tory et al. [TRM*01] present three different approaches to highlight changes in medical 4D data: semi-transparent isosurfaces colored by time; direct volume rendering encoding using intensity and change intensity over the time; glyph visualization of the change on the isosurface. The visual comparison of biomechanical motion and 3D data is proposed by Keefe et al. [KERCO9] with a mixed solution of overlay and side-by-side views assisted by a graph visualization of the change along a user selected direction. The side-by-side comparison is also used in the system VisTrails [BCC*05] to allow the user to create multiple temporal images to analyze.

Kok et al. [KBH*10] use four different visualization techniques for multi-time CT data: side-by-side, comparison by switching, overlay and a checkerboard approach using tiles from different time images. The last approach is extended by Malik et al. [MHG10] using hexagon cells to show more than two times. The visualization of statistical deformation models for 2D/3D medical images is analyzed by Caban et al. [CRY11] and Hermann et al. [HSSK16]. Caban et al. [CRY11] present four visualization algorithms: likelihood volumes to illustrate the probabilistic properties of a group of images; deformable grids to show statistical deformation properties and characterize regions with high variability; spherical glyphs to annotate the variability of different areas; line-based glyphs to illustrate deformation range and morphological variability. Hermann et al. [HSSK16] use the theory of stationary velocity fields for the interactive non-linear image interpolation and plausible extrapolation of large deformations.

To understand the spatiotemporal characteristics of time-varying volumetric data, Woodring et al. [WWS03] use a high dimensional direct rendering of a 4D data field. They utilize different integration operators and volume transfer functions to present the spatiotemporal features to the user in an intuitive manner. Caban et al. [CJR07] introduce a texture-based feature tracking technique to detect multiple features over time and find them in the following time volumes. Tracked objects are used to illustrate changes. Wang et al. [WYM08] apply an importance-driven approach to time-varying volume data visualization to enhance the identification and presentation of the essential aspects. After the computation of the importance measure, they show a system to highlight a data cluster selected by the user changing the saturation of the color fragments. Joshi et al. [JR05] show how to use some techniques inspired from the illustration literature, like speed-lines, flow ribbons, and strobe silhouettes, to help the user to see changes in the 3D volume visualization.

Some solutions have also been proposed for videos, images and 3D meshes. Wu et al. [WRS*12] propose an algorithm to magnify small changes within the same video while Balakrishnan et al. [BDG15] present a system for the comparison of two videos based on the overlays of the filtered temporal gradient. The color of the gradient edges in the final image is based on a measure of local dissimilarity. Nowell et al. [NHT01] propose a system for temporal change visualization on content collections represented as a 3D landscape. The authors investigated three techniques for drawing attention to changes from one time to the next: 3D morphing; cross-fading; a wire-frame rendering of the emerging contours superimposed on the image. Ma et al. [MXW*13] introduce a new system to synthesize changed images with desired degrees of blindness using

new metrics based on the context-dependent visual saliency and the amount of change. SimilarityExplorer [PDW*14] is a visual analysis tool for comparison of multifaceted climate models to facilitate similarity comparison tasks across both time and space. It uses the taxonomy in [GAW*11] of visual comparison methods for guiding the representation of the different aspects of similarity and the eventual placement of the different views.

In general, the existing solutions present some limitations. Some of them are not interactive, like the side-by-side approaches that make harder and time-consuming the comparison task for the user. Many techniques encode the changes in visual attributes, like the color, the color saturation, the surface bump, or employ overlapped glyphs/lines to show the differences. These approaches make difficult to understand and interpret the underlying geometric and color information of the 3D models. The main aim of our approach is to overcome such limitations.

3. Algorithm

Let us consider two 3D triangular meshes S_0 and S_1 representing the same scene at two different time steps t_0 and t_1 ($t_0 > t_1$), respectively. We assume that S_0 and S_1 are aligned, and the geometric differences have been already identified and stored in a per-vertex change field normalized in the range $[0, 1]$. This change field can be interpreted as the probability that a point on the surface has undergone a geometric change. In general, we assume that the change field is computed through a state-of-the-art method for automatic change detection. This preprocessing step should identify the regions with a significant amount of geometric differences from the ones with color differences or small geometric differences, for example due to incomplete or noisy data.

The proposed algorithm exploits the output of this change detection step, and it is based on a novel blending approach in screen-space using different temporal interpolation curves following the general insights of the studies on the *Change Blindness* phenomenon. We exploit two important observations coming out from the *Change Blindness* experiments by Simons et al. [SFR00]. This type of blindness happens when a gradual transition between the two times is used, making, in some cases, big changes less perceivable. Then the color changes are detected less often than a geometric change (for example an object that was added or removed from the scene) and their detection becomes trivial in the case of a simple instantaneous switch between the two times. These observations suggest us some hints in the design of our visualization algorithm. In particular, a smooth gradual transition for the regions identified as *no-change*, i.e. with irrelevant geometric and/or color differences, can help to reduce their perception to the user. On the other side, the trivial fast switch between the two time steps make simpler for the user to identify the significant geometric changes but, at the same time, it emphasizes all the color differences making harder the visual detection of the geometric changes. This problem is very challenging especially with models coming from image-based 3D reconstruction, where it is usual to have high-frequency shading variation due to the input photos acquired in different lighting conditions. Our approach tries to merge these observations using different interpolation curves for different regions of the 3D models to

maximize the perception of the most significant change areas and at the same time to hide the small differences in the others.

The proposed visualization algorithm computes the screen-space interpolation of the data of the 3D colored meshes S_0 and S_1 using different interpolation curves for the areas with different change values. The classification of the areas depends on a change classification threshold d , that can be selected interactively by the user. The algorithm is composed of two steps. First, we render each model independently to generate the corresponding geometry buffers where we store the normal $\vec{n}(x, y)$, the RGB color $\mathbf{c}(x, y)$ and the change value $\mathbf{q}(x, y)$ of each pixel (x, y) , generated by barycentric interpolation of the vertex info of each triangle. In the second step, we compute the screen-space interpolation of the two geometry buffers using a time variable $t \in [0, 1]$ whose value is controlled by the user with a slider. When the value of t is zero the tool shows S_0 , when $t = 1$ the tool shows S_1 , while for all the other values the tool shows a rendering obtained by a pixel-wise blending of the geometry buffer data controlled by the output of the function $\mathbf{f}_\gamma(t) : [0, 1] \rightarrow [0, 1]$. The function $\mathbf{f}_\gamma(t)$ used is a parametric smooth-step [Sch94]:

$$\mathbf{f}_\gamma(t) = \begin{cases} 1 - \frac{t}{(1/\gamma - 2)(1 - 2t) + 1} & t \leq 0.5 \\ \frac{1 - t}{(1/\gamma - 2)(2t - 1) + 1} & t > 0.5 \end{cases} \quad (1)$$

where the parameter $\gamma \in (0, 1)$ determines its shape (Figure 2a). This function has two interesting properties: for $\gamma = 0.5$ we obtain the linear function $\mathbf{f}_{0.5}(t) = 1 - t$; the functions $\mathbf{f}_\gamma(t)$ and $\mathbf{f}_{1-\gamma}(t)$ are symmetric with respect to the function $1 - t$.

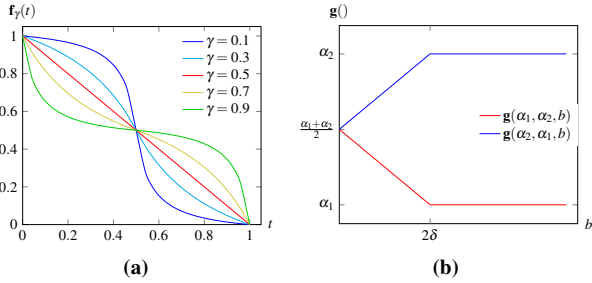


Figure 2: (a) Parametric smooth-step function \mathbf{f}_γ used for the temporal interpolation with different γ . (a) Function $\mathbf{g}(\alpha_1, \alpha_2, b)$ used for the interpolation of the blending factor near the boundary of binary classification obtained with the change threshold d .

We obtain the two different interpolation functions by using distinct shape parameters γ : γ_C for the *change* and γ_{NC} for the *no-change* regions. The evaluation of the best pair of functions to use for our purpose was done by means of a user study presented in Section 4. The outline of the algorithm is shown in Procedure 1. The input of the algorithm are the geometry buffers of the two meshes and the two alpha values $\alpha_C = \mathbf{f}_{\gamma_C}(t)$ and $\alpha_{NC} = \mathbf{f}_{\gamma_{NC}}(t)$ to use in the interpolation of change and no-change pixels. For each pixel (x, y) of the screen we recover the corresponding data from the geometry buffers of each mesh (normals $\vec{n}_0(x, y)$ and $\vec{n}_1(x, y)$,

Procedure 1 Temporal Interpolation Algorithm

Input: Geometry Buffers c, n, q for S_0 and S_1

Input: Time t , change threshold d , and light direction \vec{l}

Input: $\alpha_C = \mathbf{f}_{\gamma_C}(t)$ and $\alpha_{NC} = \mathbf{f}_{\gamma_{NC}}(t)$

Output: A dictionary \mathcal{D} of redundant patches.

```

1: for all pixel  $(x, y)$  do
2:    $\beta_C \leftarrow \mathbf{g}(\alpha_C, \alpha_{NC}, |\mathbf{q}_0 - d| + |\mathbf{q}_1 - d|)$ 
3:    $\beta_{NC} \leftarrow \mathbf{g}(\alpha_{NC}, \alpha_C, |\mathbf{q}_0 - d| + |\mathbf{q}_1 - d|)$ 
4:   if  $(\mathbf{q}_0 < d \wedge \mathbf{q}_0 \geq 0 \wedge \mathbf{q}_1 < d \wedge \mathbf{q}_1 \geq 0)$  then ▷ no change
5:      $\vec{n} \leftarrow \beta_{NC} \vec{n}_0 + (1 - \beta_{NC}) \vec{n}_1$ 
6:      $c \leftarrow \beta_{NC} \mathbf{c}_0 + (1 - \beta_{NC}) \mathbf{c}_1$ 
7:     return  $\langle c(\vec{n} \cdot \vec{l}), 1 \rangle$ 
8:   else if  $(\mathbf{q}_0 \geq 0 \wedge \mathbf{q}_1 \geq 0)$  then ▷ change
9:      $c \leftarrow \beta_C \mathbf{c}_0(\vec{n}_0 \cdot \vec{l}) + (1 - \beta_C) \mathbf{c}_1(\vec{n}_1 \cdot \vec{l})$ 
10:    return  $\langle c, 1 \rangle$ 
11:   else if  $(\mathbf{q}_0 \geq 0)$  then ▷ only  $S_0$ 
12:     return  $\langle \mathbf{c}_0(\vec{n}_0 \cdot \vec{l}), \beta_C \rangle$ 
13:   else if  $(\mathbf{q}_1 \geq 0)$  then ▷ only  $S_1$ 
14:     return  $\langle \mathbf{c}_1(\vec{n}_1 \cdot \vec{l}), 1 - \beta_C \rangle$ 
15:   return  $\langle \text{black}, 0 \rangle$ 
    
```

colors $\mathbf{c}_0(x, y)$ and $\mathbf{c}_1(x, y)$, change values $\mathbf{q}_0(x, y)$ and $\mathbf{q}_1(x, y)$). This data are used to classify the pixel as change or no-change and to determine the type of interpolation to apply. A screen pixel is classified as no change only if both the meshes project on that pixel a value $\mathbf{q}(x, y)$ below the selected change classification threshold d . If at least one mesh projects a value $\mathbf{q}(x, y)$ above d the pixels is classified as change. In the other cases, where only one mesh projects geometry on the pixel, due for example to data not acquired in the other time, the pixel is classified as change (in this case, the time with no information return a negative value $\mathbf{q}(x, y)$). The next step is the interpolation of the data. For the no-change pixels, we calculate the alpha blending of the two normals and colors independently and then we compute the final Lambertian shading with the interpolate values. The computation of the blending of normals and colors before the shading permits to partially hide negligible variations like high frequency geometric and color differences due to non-relevant factors (see the additional video). Instead for the change pixel, we compute independently the Lambertian shading of each time and then we blend the computed shaded colors. For the pixel with a single valid time, we blend the shaded color with the background color of the screen.

The use of a binary classification between the change and no-change areas and the choice of the respective interpolation functions with different parameters γ can produce visible rendering artifacts near the boundary of the classification (see Figure 3 for an example). To overcome this problem we interpolate the alpha parameters α_C and α_{NC} in a neighborhood of the change threshold d . For this purpose we require a change field with a continuous and smooth radial distribution around the real changes, like the field computed with a simple Hausdorff distance or with [PCBS16]. In particular, for all the pixels with at least one change value \mathbf{q}_0 and \mathbf{q}_1 in the range $[d - \delta, d + \delta]$ we interpolate the alpha blending parameters using the following function $\mathbf{g}(\alpha_1, \alpha_2, |\mathbf{q}_0 - d| + |\mathbf{q}_1 - d|)$

(Figure 2b):

$$\mathbf{g}(\alpha_1, \alpha_2, b) = \begin{cases} \frac{\alpha_1 + \alpha_2}{2} + \frac{(\alpha_1 - \alpha_2)}{2} \frac{b}{2\delta} & b \leq 2\delta \\ \alpha_1 & b > 2\delta \end{cases} \quad (2)$$

The obtained result is a smoother transition near the boundary of the binary segmentation that makes less abrupt and more pleasant the final color interpolation (Figure 3). The parameter δ determines the extension of the interpolation around the boundary of the binary classification and its value depends on the algorithm used to compute the change field and in particular on the distribution of the change value in the range $[0, 1]$. In all our experiments we used always the same value $\delta = 0.15$ assuming a linear distribution of the normalized change field.

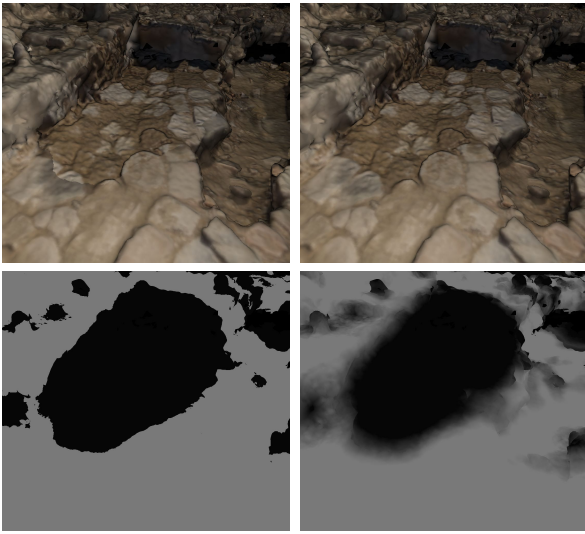


Figure 3: Results obtained without (left) and with (right) the use of the interpolation of α_c and α_{nc} with the function $\mathbf{g}(\alpha_1, \alpha_2, b)$. The bottom row shows the corresponding weight map used for the final blending of the meshes. ($t = 0.8$, $\alpha_c = \mathbf{f}_{0.05}(t)$ and $\alpha_{nc} = \mathbf{f}_{0.95}(t)$, $d = 0.3$, $\delta = 0.15$).

4. User study

In this section, we present the results of the user study conducted to evaluate the effectiveness of the proposed technique. The user study is subdivided into three sessions. In the first one (Section 4.3), we evaluate the effectiveness of the technique from an objective point of view. For this purpose, we asked the subjects to perform a visual task and we measured the performance obtained with four different approaches. In the second session (Section 4.4), we evaluate our technique in a subjective manner. We showed different scenes and we asked the user to score how much effective are four different visualization techniques in showing the visual differences. In the third session (Section 4.5), we compared the proposed techniques with the direct visualization of the binary change map. We asked to detect a subset of occurred changes and we measured the accuracy of the detection and the completion time.

At the begin of each session, we make a training phase where the subject is instructed with the task to perform. When we show the different scenes we use fixed viewpoints, the user cannot navigate inside the 3D scene. This choice has been done to guarantee uniform conditions of use between the subjects avoiding that the way a user navigates the 3D model influences the evaluation of the different techniques. During the first test, an automatic animation between the two time instants is employed. Instead, during the second and the third tests the user can interact freely with the slider control. A complete description of the protocol used in the tests, the details of the data analysis conducted, and the aggregated results of the three sessions are reported in the Additional Material.

4.1. Dataset

In the first two sessions, we used six datasets with different characteristics and created with different reconstruction techniques. Figure 4 shows the 11 viewpoints used in the user study with the relative data (threshold d for the change/no-change classification and size in million of triangles). The value of the threshold d is dataset dependent and it needs some initial tuning that can be done in real-time inside the visualization tool. We have four datasets created by multi-view reconstruction from photos: ST.MARTA an archaeological excavation; PARIS a Roman Arena in Paris; SEAWEED a pile of seaweed on the beach; and GROUND some piles of ground in a construction site acquired in three different times. In general, the meshes have some inconsistency with high frequency color and geometric variations due to the different lighting conditions during the photographic campaign. These models are also noisy and can have parts at different resolution due to the acquisition process. The other two datasets (OFFICE and LAB) show two different rooms, an office and a lab, acquired with a Time-of-Flight (ToF) scanner and subsequently triangulated. In these datasets, the acquisition noise is very low and the meshes present only large geometric changes due to objects' movements. For the third session, we created two synthetic terrain datasets characterized by geometric and color changes. Figure 5 shows the viewpoints used in the user study.

To detect the changes between the input meshes, we use a variant of the method presented in [PCBS16]. The algorithm computes a multi-scale Growing Least Square (GLS) [MGB*12] descriptor, independently for each mesh, with an adaptive subsampling of the volume occupied by the models using an octree. This permits to adapt the density of the descriptors with the point density of the meshes. Then we map the differences of these descriptors in the time over the original models. The final result is a per-vertex change field in the range $[0, 1]$ that can be interpreted as a change probability. The computed field shows an amount of smoothness (top row in Figure 12) that can reduce the rendering artifacts around the transition between change and no-change regions.

4.2. Techniques

In the first two sessions we compare four techniques: switch between images (SWITCH), linear blending (LINEAR), and two variants of the proposed technique (SMOOTHSTEP1 and SMOOTHSTEP2). The switch (SWITCH), or instantaneous alternation, between the different scenes, has been chosen because is the typical

	S_0	S_1	Change Map S_0	Change Map S_1	Param
ST.MARTA1					$d = 0.3$ $S_0 = 7.1M$ $S_1 = 10M$
ST.MARTA2					$d = 0.3$ $S_0 = 7.1M$ $S_1 = 10M$
ST.MARTA3					$d = 0.3$ $S_0 = 7.1M$ $S_1 = 10M$
PARIS1					$d = 0.4$ $S_0 = 7M$ $S_1 = 24.2M$
OFFICE					$d = 0.05$ $S_0 = 18.4M$ $S_1 = 17.9M$
LAB1					$d = 0.05$ $S_0 = 18.6M$ $S_1 = 18.5M$
LAB2					$d = 0.05$ $S_0 = 18.6M$ $S_1 = 18.5M$
SEAWEED1					$d = 0.5$ $S_0 = 18.2M$ $S_1 = 13.6M$
SEAWEED2					$d = 0.5$ $S_0 = 18.2M$ $S_1 = 13.6M$
GROUND1					$d = 0.3$ $S_0 = 9.8M$ $S_1 = 16.5M$
GROUND2					$d = 0.3$ $S_0 = 19.5M$ $S_1 = 16.5M$

Figure 4: Viewpoints of the real datasets used in the first and second user studies (Sections 4.3 and 4.4). Each viewpoint shows the two times, the relative change maps computed with [PCBS16] (blue = no-change, red = change), the parameter d for the change/no-change classification and the size of the two meshes in million of triangles.

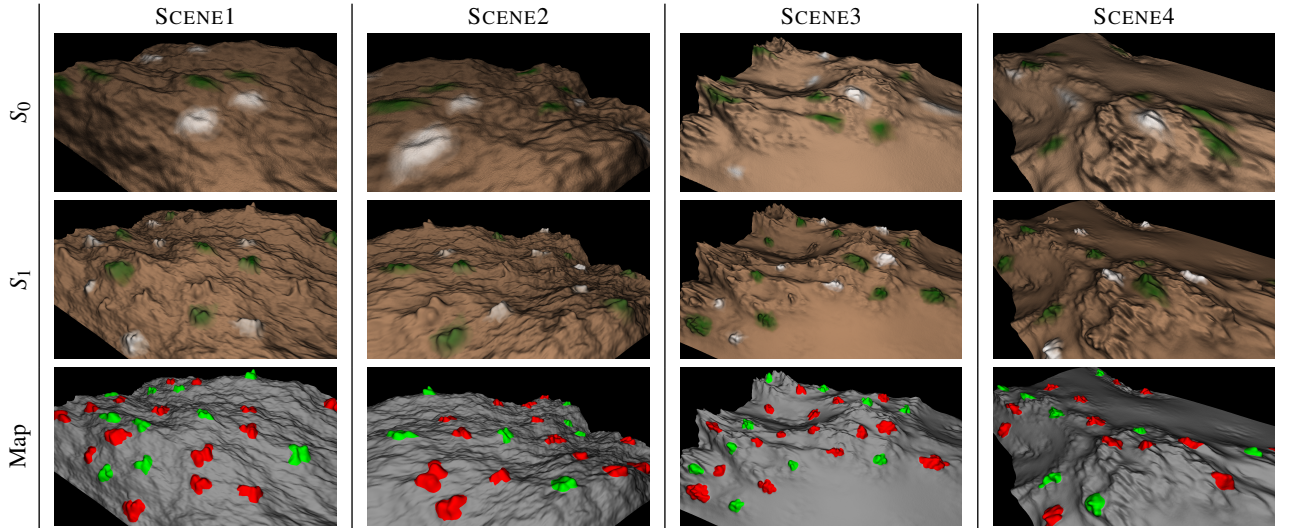


Figure 5: Viewpoints of the synthetic datasets used in the third user study (Section 4.5). Each viewpoint shows the two times (S_0 and S_1) and the change map with the classification of the change regions that should be marked in the test (green = change to mark, red = change to not mark, gray = no-change).

way of comparing different images inside all the software that use layers. For example, many image processing, image editing, and GIS software tools use layers to show different information or different parts of overlapping images. The linear blending (LINEAR) has been selected to understand if this simple mix of the scenes allows the subject to interpret well the scene changes. The two variants of the proposed method follow the main principles but have different properties explained below. Note that, all of these techniques can be implemented using interpolation functions of different shapes (see Figure 6). The SWITCH and LINEAR techniques use the same function for both the change/no-change categories ($\mathbf{f}_{\gamma_c}(t) = \mathbf{f}_{\gamma_{NC}}(t)$). We implement the SWITCH with an instantaneous transition from one time to the next at the time $t = 0.5$. The LINEAR method is implemented with a function with parameter $\gamma_c = \gamma_{NC} = 0.5$. The first variant of the proposed method (SMOOTHSTEP1) uses a linear blending for the no-change regions ($\gamma_{NC} = 0.5$) and a smooth-step interpolation for the change areas ($\gamma_c = 0.05$). The second variant of the method (SMOOTHSTEP2) uses a smooth-step interpolation for both the classes with two different symmetric functions ($\gamma_c = 0.05$ and $\gamma_{NC} = 0.05$). The main difference of these methods is in the perception of the no-change regions. In the method SMOOTHSTEP1 the no-change regions are interpolated in a linear way avoiding abrupt color changes that can make small differences perceivable. At the same time, the change regions appear quickly in the central times around $t = 0.5$. In the method SMOOTHSTEP2 the interpolation of the no-change regions happens in two separated moments, near $t = 0$ and $t = 1$ in a fast way, while it stays completely still during the interpolation of the change areas (around $t = 0.5$). In this way, we try to minimize distraction factors when the change is shown. For both the techniques the value of the parameter $\gamma_c = 0.05$ is selected following the insights of the Change Blindness experiments where emerge that a fast transaction between the two time steps make simpler for the user to identify the significant visual changes. For this reason, we select a value that

makes enough close the function $\mathbf{f}_{\gamma_{NC}}(t)$ to an instantaneous switch but that avoids the creation of rendering artifacts near the boundary of the binary classification thanks to its continuity. To validate this choice we conducted a specific user study with the same protocol of the second test (Section 4.4). We asked 11 users to score from 1 (bad) to 5 (good) how much effective in showing the visual differences are four versions of the method SMOOTHSTEP1 using different values of γ_c . The results obtained are in line with our expectation and validates the choice of $\gamma_c = 0.05$. Indeed, we obtain: MS=1.891 (1.188) for $\gamma_c = 0.5$ (like the method LINEAR), MS=2.455 (0.902) for $\gamma_c = 0.35$, MS=3.527(0.904) for $\gamma_c = 0.15$ and MS=4.527 (0.467) for $\gamma_c = 0.05$. MS stands for mean score, the value in parenthesis is the corresponding variance.

4.3. Objective evaluation

To evaluate the effectiveness of the approach we measure how well the subjects are able to correctly identify *change/no-change* areas in a number of scenes by tagging squares of a superimposed grid. Each test consists of one of the eleven viewpoints previously shown in Figure 4. A technique from the four under investigation is chosen randomly and used for each user/scene combination. The subject sees an automatic transition from S_0 to S_1 and back to S_0 , performed in 5 seconds. This animation is repeated 3 times. The length of the animation is sufficient to activate the visual working memory [War04] and, at the same time, such that the velocity of the visual transitions of the changes can capture the visual attention of the users (i.e. the change blindness phenomenon). The number of repetition permits the subject to better localize the changes. Three repetitions make the total session duration reasonable. At the end of the third animation, the subject can indicate the *change/no-change* regions on a superimposed 7 grid by tagging each tile as change (red tile) or no-change area (blue tile). The tiles for which the subject is uncertain should remain untagged and are recorded as “no answer” (Figure 7). We did not use the available change/no-change

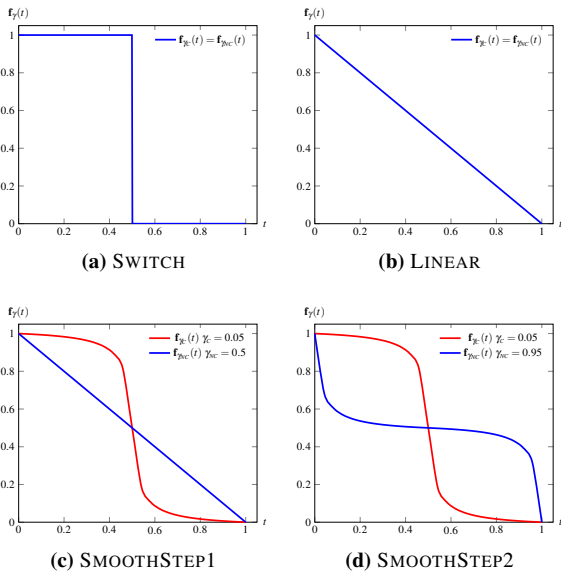


Figure 6: Shape of the interpolation functions f_C and f_{NC} used by the four techniques tested in the user study.

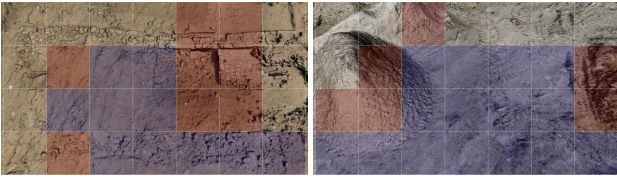


Figure 7: GUI used in the objective evaluation with an example of user input. Red tiles indicate perceived changes, blue tiles indicate no changes. No input indicates that the user has no a clear choice for that tiles.

segmentation for the tagging to not provide any information to the user on the location of the change. The size of the grid has been chosen to complete the test in reasonable time.

Concerning the type of changes, we asked to indicate *significant* geometric difference avoiding non-relevant geometric changes due for example to different precision in the acquisitions. To better assess what significant differences are, during the instruction phase we mentioned explicitly to indicate objects or parts of the scene that appear or disappear or parts of the scene that change their shape significantly. Since we design our technique with the goal to “hide” minor/moderate color changes we deliberately not mentioned anything about color differences. Consider that an evaluation of the selected scenes with the HDR-VDP [MKRH11] proved that all the parts of the scenes have noticeable visual differences. Hence, the task to indicate the significant change is difficult.

Twenty-one volunteers participated in the test (age ranges from 30 to 52, 75% male, 60% computer scientists). The data have been aggregated measuring, for each technique, the tiles correctly identified as “change” (C), the tile correctly identified as “no-change” (NC) and the “no answered” tiles (NA). We compute the

weights $w_C = \min(1, \frac{2a}{c})$ for each tile indicated as change and $w_{NC} = \min(1, \frac{2b}{c})$ for each tile indicated as no-change, where c is the number of pixels in the tile where at least one mesh projects geometry, a is the number of these pixels classified as change and b is the number of pixel classified as no-change. For the pixel classification we use the same approach in Algorithm 1: a pixel is no-change iff both the models project a change value q below the segmentation threshold d on the pixel; for all the other cases the pixel is classified as change. The final values C are computed as average of w_C of all the tiles indicated as change for the technique (the same for the values NC). Instead, NA is simply the percentage of tiles with no answers provided. The results for each technique are summarized in Table 1 (means and variances for C and NC , the unknown rate NA and the absolute number of tile for each categories #Tiles). See the additional material for the data aggregated by subject and scene.

From these results, it is possible to note that, despite the intrinsic difficulty of the task requested, the subjects are quite good to identify changes between the scenes. The SWITCH technique is the one that performs poorly. Instead, the other three methods have similar performance for the value C and NC even if the SMOOTHSTEP1 technique is quite better in reducing the number of tiles that received “no answer”. This means that the SMOOTHSTEP1 method helps more the subject to understand where the changes are. This is confirmed by the higher number of tiles (column #Tiles) indicated by the subjects as change (478), which is the 36% higher than LINEAR and 16% higher than SMOOTHSTEP2. A better evaluation can be done by computing a global score for the detection of change and no change considering the unknown rate NA . This score is reported in the columns #Score for the change and the no-change in the Table 1. Its value is obtained by computing for each single test two performance parameters: the right change score and the right no-change score of the test weighted with the percentage of tiles with an answer. These per-test scores are aggregated for each technique. In this way, the contribution of a subject with a test with few no-answer tiles is higher in the computation of the final score. This global score indicates that the technique SMOOTHSTEP1 performs better than the others methods. To evaluate the significance of these results we performed a hypothesis test on the scores obtained evaluating the alternative hypothesis that the mean score of the technique X is greater than the mean score of the technique Y. We obtain that SMOOTHSTEP1 is effectively better than SWITCH and LINEAR for identify changes (p-value=0.0043 and 0.0495 respectively). Regarding the no change regions SMOOTHSTEP1 is still significantly better than the SWITCH (p-value=0.0016) while the null hypothesis cannot be rejected at significance level of 5% for the LINEAR method (p-value=0.111, that, however is a low value). Hence, in general, we can state that SMOOTHSTEP1 performs better than the other techniques.

4.4. Subjective evaluation

In this test, the subject is instructed to test the different visualization techniques directly and rate them with a score from 1 to 5 according to his/her preference. In this experiment, the subject knows the change/no-change segmentation of the scene. The change map is displayed on a side monitor during the interactive session with a

	Change			NC	No-Change		No-Answer	
	C	#Tiles	Score		#Tiles	Score	NA	#Tiles
SWITCH	0.680(0.136)	437	0.369(0.072)	0.931(0.043)	421	0.415(0.129)	0.46	730
LINEAR	0.758(0.107)	351	0.409(0.100)	0.923(0.051)	643	0.527(0.134)	0.374	595
SMOOTHSTEP1	0.738(0.109)	478	0.497(0.060)	0.958(0.027)	600	0.606(0.099)	0.319	506
SMOOTHSTEP2	0.729(0.118)	410	0.420(0.076)	0.929(0.049)	507	0.409(0.118)	0.412	643

Table 1: Results from the objective evaluation session. All the techniques are almost equally efficient for the identification of the scene changes with the exception of SWITCH. The method SMOOTHSTEP1 performs better than the other two methods yielding a lower number of no-answer (NA) and a higher number of correct change tiles detected ($0.738 \times 478 = 352.7$ tiles). This is confirmed by the global score for change 0.497 and no-change 0.606. The numbers in parenthesis are the corresponding variances.



Figure 8: GUI used in the subjective evaluation. (Top) Main monitor. For each technique, the subject can interact with the corresponding slider to evaluate its effectiveness in the visualization of the geometric differences. (Bottom) Monitor layout. A false color map is shown on a monitor close to the one in front of the subject.

false color map (see Figure 8). All the techniques were visualized simultaneously so that the subject can better appreciate the different effects produced. We asked to evaluate with '1' the techniques that are not effective to show the changes and with '5' the techniques that are very effective. We asked also to take into account the effectiveness in hiding the no-change parts of the scene. The subject evaluates the techniques by moving the time slider provided for each technique. For this session we selected five viewpoints from the ones in Figure 4 (ST.MARTA1, ST.MARTA2, OFFICE, SEAWEED1, and GROUND1).

Twenty-four volunteers participated in the test (age ranges from 30 to 52, 75% male, 60% computer scientists). We analyzed the collected scores to identify and remove scoring bias. By aggregating the scores for each technique and performing an analysis-of-variance (ANOVA) we found that a simple mean normalization [Gui54] of the scores is sufficient to remove differences across sub-

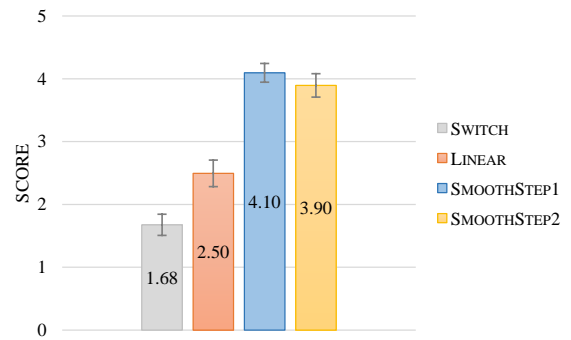


Figure 9: Subjective evaluation. Average scores and 95% confidence intervals of the four tested techniques without the subjects detected as outliers. Note the high preference of the methods SMOOTHSTEP1 and SMOOTHSTEP2 w.r.t to the other techniques.

jects. These scores had been also analyzed using a Kurtosis analysis in order to identify a range of values for which a subject can be considered an outlier and then screened. The screening procedure follows the Annex 2 of ITU BT.500 Recommendation [Uni02]. According to this procedure, we found that 3 of 24 subjects have may be outliers, so they were removed from the final analysis. Figure 9 shows a chart with the average scores and the relative 95% confidence interval. Figure 10 shows the scores aggregated for each scene. The additional material contains the tables with the scores (average and variance) aggregated for each technique and for each scene with and without outliers screening.

The results in Figure 9 and Figure 10 show that for the user the most effective method for the visualization of the geometric differences is SMOOTHSTEP1 (highest score and lowest variance). The method SMOOTHSTEP2 has a slightly worse rate but is almost as effective as SMOOTHSTEP1. We argue that its lower score is due to the no-change interpolation function that makes clearly noticeable minimum color differences between the meshes at the beginning and at the end of the slider. This features can disturb the user especially in the datasets with high color variation, like SEAWEED1 and GROUND1. On the contrary, the method LINEAR presents a very low score despite its good performance in the objective evaluation. The method SWITCH confirms the bad performance already emerged in the first session.

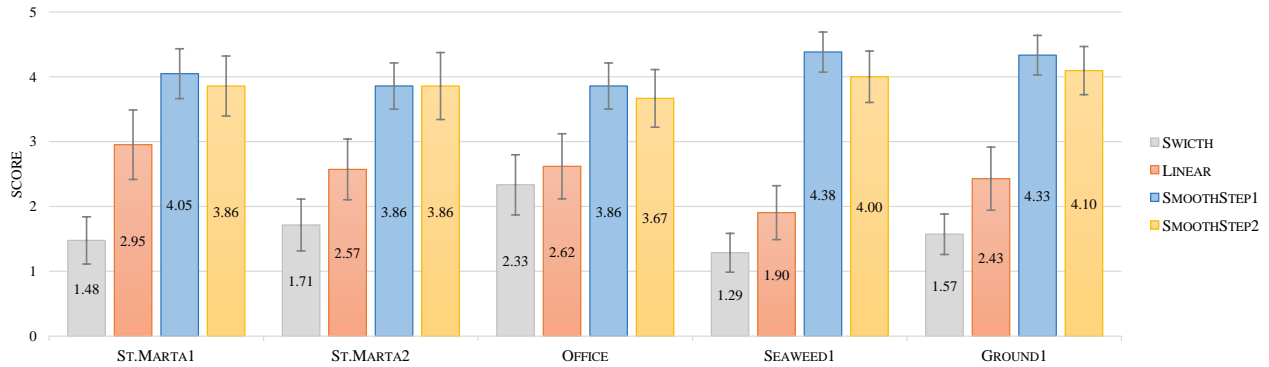


Figure 10: Subjective evaluation. Average scores and 95% confidence intervals of the four tested techniques aggregated for each scene without the subjects detected as outliers. The methods SMOOTHSTEP1 and SMOOTHSTEP2 are the most effective in each tested scene with a slightly higher preference for the method SMOOTHSTEP1.

Finally using the Kolmogorov-Smirnov (KS) test, we can reject the null hypotheses that the pairs SWITCH-LINEAR ($p = 6.94 \times 10^{-7}$), SWITCH-SMOOTHSTEP1 ($p = 1.97 \times 10^{-29}$), SWITCH-SMOOTHSTEP2 ($p = 3.25 \times 10^{-23}$), LINEAR-SMOOTHSTEP1 ($p = 1.35 \times 10^{-12}$) and LINEAR-SMOOTHSTEP2 ($p = 1.06 \times 10^{-9}$) are from the same distribution. On the contrary, the pair SMOOTHSTEP1-SMOOTHSTEP2 are strictly correlated ($p = 0.78$) as we expect. This correlation is also indirectly confirmed by the opinions of the subjects at the end of the second session where many people declared that SMOOTHSTEP1 and SMOOTHSTEP2 are in general similar and hard to distinguish.

4.5. Comparison with the direct change map visualization

In this session, we compared the proposed technique SMOOTHSTEP1 with a method based on the direct visualization of a binary change map. We refer to this method with CHANGEMAP in the following. We asked the subject to complete a detection task of the main geometric changes in a scene that, at the same time, are not characterized by a significant color change. We used the viewpoints of the synthetic terrain datasets depicted in Figure 5. The subject interacted by moving the time slider to go from one time to the other. For the method CHANGEMAP the slider permit to switch from one instant time to another one. When the CHANGEMAP method is used, the user can also switch on the change map visualization by pressing a button on the keyboard. During the change map visualization, the subject cannot mark the change regions and interact with the time slider. The subject can mark the change regions with a double click inside the area of the screen interested by the change in any time. The marked positions are indicated by a small circle. During the training phase, we showed some example of changes that should (without a big color change) and should not (with a big color change) be marked. Twelve volunteers participated in the test (age ranges from 25 to 40, 75% are male, 85% are computer scientists). For each test, we collected all the marks entered by the subject. We registered also the elapsed time from the beginning of the test when each mark was entered. We classify as right all the marks at less of 10 pixels far from a geometric change region with no significant color change. Figure 11 shows the trend of the num-

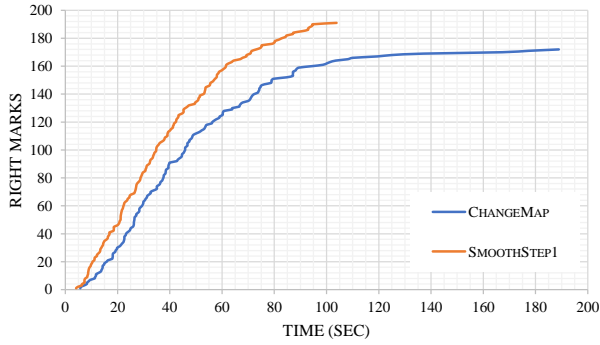
ber of right marks versus the elapsed time for both the methods and a table with the number of right and wrong marks at different times of the test. The wrong marks are indicated in parenthesis. According to these results, we can state that the SMOOTHSTEP1 allows the user to detect a greater number of changes in a faster way (the curve of the aggregate number of right marks vs time is always above the ones for the CHANGEMAP) with a limited loss of accuracy (6 wrong marks against 2).

5. Web Visualization Tool

The proposed visualization technique has been implemented as a web application for real-time exploration of triangular mesh on the web. To allow the real-time interaction with the 3D models, the application employs the multi-resolution structure defined in [CGG*05]. For this reason, the two 3D models require a pre-processing to compute an 8-bit quantization of the change field to store in the alpha channel of the per-vertex color and then a further processing to create the multi-resolution structure. The tool allows the classical 3D navigation using a trackball paradigm with a simple slider control to navigate the two models in the time. Then the tool provides some additional options, like the possibility to try all the techniques tested in the user study, to change the classification threshold d , to show the mapping of the change field in different color maps. The code of the tool with some datasets are available at the following link <http://vcg.isti.cnr.it/~palma/visChange/>.

6. Discussion and Extensions

The results of the user study show how much a simple method like the technique SMOOTHSTEP1 can be very effective in the visualization of 3D geometric differences in the time. A current requirement of the method is to have in input a pre-computed per-vertex change field with a consistent meaning around the geometric changes and with smooth values in the range $[0, 1]$. Obviously, the choice of the change detection algorithm can partially influence the effectiveness of the method, even if the principles behind it still remains valid. In the released visualization tool we add a demo with



	Time				
	20s	40s	60s	80s	End
CHANGEMAP	30 (0)	90 (2)	124 (2)	151 (2)	172 (2)
SMOOTHSTEP1	46 (2)	113 (5)	157 (5)	176 (5)	191 (6)

Figure 11: Graph of the aggregated number of the right marks on the change areas in function of the elapsed time of the test. The bottom table shows the number of right marker at several times of the test (in parenthesis the wrong marks). The results show how the method SMOOTHSTEP1 allows the subject to note more changes in less time with respect to the method CHANGEMAP with a limited loss of accuracy.

two different versions of a Gargoyle where the change field was computed with different algorithms: the algorithm from [PCBS16] and the Hausdorff distance [CRS98] normalized with respect to the maximum distance. The relative change maps are shown in Figure 12. Even if the Hausdorff distance can create more noise on the change fields, the effectiveness of the method is only partially influenced and some of the related problems can be solved with a pre-filtering of the computed change field.

An interesting feature of the method is the fact that works in screen-space processing each pixel independently. This makes the method very generic, for example, it can be directly applicable to change maps obtained at object-level instead of at surface point level. In this case the pre-processing tracks the objects movements inside the 3D scene. Additionally, working in screen-space permits to adopt the proposed approach to other inputs, like 2D images or 3D volume. We leave this extension as an interesting matter of future research.

An intrinsic limitation of the proposed approach is that it is not suitable to show changes that cannot be perceived visually. For example, a smooth deformation of a geometry along the view direction is not easy to perceive visually. In this case, our interpolation scheme does not help to make this change more understandable and distinguishable. Instead, a false color map can show that all the scene is slightly changed. In some cases, this limitation can be overcome by changing the viewpoint or the zooming factor of the camera that inspects the virtual scene.

7. Conclusion

We have proposed a new real-time visualization technique to enhance the understanding of the 3D temporal geometric changes of

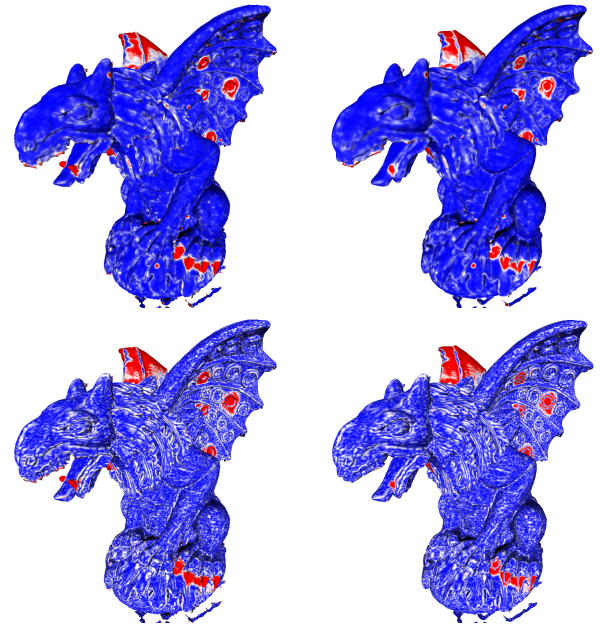


Figure 12: Blue-White-Red color mapping of the $[0..1]$ change field on the two meshes S_0 (left) and S_1 (right) computed with two different methods: (top) [PCBS16]; (bottom) [CRS98]. Note how direct color-mapping can worsen the readability of the 3D model shape making difficult to perceive the actual geometric difference between the left and right models.

an evolving scene. Starting from a change/no-change segmentation of two input 3D meshes, the method computes a screen-space interpolation of the two geometry buffers using different interpolation curves according to the classification. By exploiting the insights of the cognitive experiments on *Change Blindness*, we have designed two different interpolation functions that are able to improve the perception of the most significantly changed regions and, at the same time, to hide the negligible, yet visually noticeable, color and geometric differences due to noise and high-frequency variations (small acquisition imperfections, color shading variation due to different lighting, small scale changes). To assess the effectiveness of the proposed approach we conducted a user study. We evaluated two variants of the technique SMOOTHSTEP1 and SMOOTHSTEP2 against a simple fast switch and a linear blending visualization. The results of the user study show that the proposed methods are the most effective and the most preferred techniques. More precisely, the objective evaluation shows that the method SMOOTHSTEP1 is the most efficient in helping the subject to understand where the changes are located with less uncertainty (it has the lowest number of areas with no answer). The method SMOOTHSTEP1 received the highest score with the lowest variance also in the subjective evaluations. The proposed method is very simple to implement, has a negligible impact on the rendering time and it can be easily integrated into an existing rendering system. To demonstrate these strength points, we have released an interactive web application (<http://vcg.isti.cnr.it/~palma/visChange>).

8. Acknowledgment

We acknowledge the partial support of the project D-Surf (PRIN 2015B8TRFM), funded by the Ministry of Education, University and Research (MIUR), and of the project SCIADRO, co-funded by the Tuscany Region (Italy) under the Regional Implementation Programme for Underutilized Areas Fund (PAR FAS 2007-2013) and the Research Facilitation Fund (FAR) of the Ministry of Education, University and Research (MIUR). We thank the anonymous reviewers for their constructive comments and the Prof. Stefano Campana for the ST. MARTA dataset.

References

- [BCC*05] BAVOIL L., CALLAHAN S. P., CROSSNO P. J., FREIRE J., SCHEIDEGGER C. E., SILVA C. T., VO H. T.: VisTrails: enabling interactive multiple-view visualizations. In *Visualization, 2005. VIS 05. IEEE* (Oct 2005), pp. 135–142. [3](#)
- [BDG15] BALAKRISHNAN G., DURAND F., GUTTAG J.: Video Diff: Highlighting Differences Between Similar Actions in Videos. *ACM Trans. Graph.* **34**, 6 (Oct. 2015), 194:1–194:10. [1](#), [3](#)
- [CGG*05] CIGNONI P., GANOVELLI F., GOBBETTI E., MARTON F., PONCHIO F., SCOPIGNO R.: Batched Multi Triangulation. In *VIS 05. IEEE Visualization, 2005.* (Oct 2005), pp. 207–214. [10](#)
- [CJR07] CABAN J., JOSHI A., RHEINGANS P.: Texture-based Feature Tracking for Effective Time-varying Data Visualization. *IEEE Trans. Vis. Comput. Graphics* **13**, 6 (Nov. 2007), 1472–1479. [3](#)
- [CRS98] CIGNONI P., ROCCHINI C., SCOPIGNO R.: Metro: Measuring error on simplified surfaces. *Computer Graphics Forum* **17**, 2 (1998), 167–174. [11](#)
- [CRY11] CABAN J. J., RHEINGANS P., YOO T.: An Evaluation of Visualization Techniques to Illustrate Statistical Deformation Models. In *Proc. EuroVis* (Chichester, UK, 2011), EuroVis'11, The Eurographics Association, pp. 821–830. [1](#), [3](#)
- [GAW*11] GLEICHER M., ALBERS D., WALKER R., JUSUFI I., HANSEN C. D., ROBERTS J. C.: Visual Comparison for Information Visualization. *Information Visualization* **10**, 4 (Oct 2011), 289–309. [2](#), [3](#)
- [Gui54] GUILFORD J.: *Psychometric methods*. McGraw-Hill series in psychology. McGraw-Hill, 1954. [9](#)
- [HSSK16] HERMANN M., SCHUNKE A. C., SCHULTZ T., KLEIN R.: Accurate interactive visualization of large deformations and variability in biomedical image ensembles. *IEEE Trans. Vis. Comput. Graphics* **22**, 1 (2016), 708–717. [3](#)
- [JR05] JOSHI A., RHEINGANS P.: Illustration-inspired techniques for visualizing time-varying data. In *Visualization, 2005. VIS 05. IEEE* (Oct 2005), pp. 679–686. [3](#)
- [KBH*10] KOK P., BAIKER M., HENDRIKS E. A., POST F. H., DIJKSTRA J., LOWIK C. W. G. M., LELIEVELDT B. P. F., BOTHA C. P.: Articulated Planar Reformation for Change Visualization in Small Animal Imaging. *IEEE Trans. Vis. Comput. Graphics* **16**, 6 (Nov 2010), 1396–1404. [1](#), [3](#)
- [KER09] KEEFE D., EWERT M., RIBARSKY W., CHANG R.: Interactive Coordinated Multiple-View Visualization of Biomechanical Motion Data. *IEEE Trans. Vis. Comput. Graphics* **15**, 6 (Nov. 2009), 1383–1390. [3](#)
- [LFM*13] LI Y., FAN X., MITRA N. J., CHAMOVITZ D., COHEN-OR D., CHEN B.: Analyzing Growing Plants from 4D Point Cloud Data. *ACM Transaction on Graphics* **32**, 6 (Nov. 2013), 157:1–157:10. [1](#)
- [LLD*97] LOOMIS J. J., LIU X., DING Z., FUJIMURA K., EVANS M. L., ISHIKAWA H.: Visualization of plant growth. In *Proc. Visualization* (Oct 1997), pp. 475–478. [2](#)
- [LLV*00] LEEUW W. C. D., LIERE R. V., VERSCHURE P. J., VISSER A. E., MANDERS E. M. M., DRIELF R. V.: Visualization of time dependent confocal microscopy data. In *Proc. Visualization* (Oct 2000), pp. 473–476. [2](#)
- [MGB*12] MELLADO N., GUENNEBAUD G., BARLA P., REUTER P., SCHLICK C.: Growing Least Squares for the Analysis of Manifolds in Scale-Space. *Computer Graphics Forum* **31**, 5 (2012), 1691–1701. [5](#)
- [MHG10] MALIK M. M., HEINZL C., GROELLER M. E.: Comparative Visualization for Parameter Studies of Dataset Series. *IEEE Trans. Vis. Comput. Graphics* **16**, 5 (Sept 2010), 829–840. [3](#)
- [MKRH11] MANTIUK R., KIM K. J., REMPEL A. G., HEIDRICH W.: Hdr-udp-2: A calibrated visual metric for visibility and quality predictions in all luminance conditions. *ACM Trans. Graph.* **30**, 4 (2011), 40:1–40:14. [8](#)
- [MXW*13] MA L. Q., XU K., WONG T. T., JIANG B. Y., HU S. M.: Change Blindness Images. *IEEE Trans. Vis. Comput. Graphics* **19**, 11 (Nov 2013), 1808–1819. [3](#)
- [NHT01] NOWELL L., HETZLER E., TANASSE T.: Change blindness in information visualization: a case study. In *Proc. INFOVIS* (2001), pp. 15–22. [3](#)
- [PCBS16] PALMA G., CIGNONI P., BOUBEKEUR T., SCOPIGNO R.: Detection of geometric temporal changes in point clouds. *Computer Graphics Forum* **35**, 6 (2016), 33–45. [1](#), [4](#), [5](#), [6](#), [11](#)
- [PDW*14] POCO J., DASGUPTA A., WEI Y., HARGROVE W., SCHWALM C., COOK R., BERTINI E., SILVA C.: SimilarityExplorer: A Visual Inter-Comparison Tool for Multifaceted Climate Data. *Computer Graphics Forum* (2014). [3](#)
- [PM07] POLLARD T., MUNDY J. L.: Change Detection in a 3-d World. In *IEEE Conference on Computer Vision and Pattern Recognition* (Minneapolis, 2007), IEEE, pp. 1–6. [1](#)
- [PP95] PAGENDARM H., POST F.: *Comparative Visualization: Approaches and Examples*, vol. 95 of *Reports of the Faculty of Technical Mathematics and Informatics*, Delft University of Technology. Delft University of Technology, 1995. [1](#), [2](#)
- [Sch94] SCHLICK C.: Fast Alternatives to Perlin's Bias and Gain Functions. In *Graphics Gems IV*, Heckbert P. S., (Ed.). Academic Press Professional, Inc., San Diego, CA, USA, 1994, pp. 401–403. [4](#)
- [SFR00] SIMONS D. J., FRANCONERI S. L., REIMER R. L.: Change blindness in the absence of a visual disruption. *Perception* **29**, 10 (2000), 1143–1154. [2](#), [3](#)
- [Sim00] SIMONS D. J.: Current Approaches to Change Blindness. *Visual Cognition* **7**, 1-3 (2000), 1–15. [2](#)
- [SL97] SIMONS D. J., LEVIN D. T.: Change blindness. *Trends in cognitive sciences* **1**, 7 (1997), 261–267. [2](#)
- [TBP13] TANEJA A., BALLAN L., POLLEFEYS M.: City-Scale Change Detection in Cadastral 3D Models Using Images. In *IEEE Conference on Computer Vision and Pattern Recognition* (Columbus, 2013), IEEE, pp. 113–120. [1](#)
- [TRM*01] TORY M., RÖBER N., MÖLLER T., CELLER A., ATKINS M. S.: 4D Space-time Techniques: A Medical Imaging Case Study. In *Proc. Visualization* (Washington, DC, USA, 2001), VIS '01, IEEE Computer Society, pp. 473–476. [1](#), [3](#)
- [Uni02] UNION I. T.: ITU-T Rec. BT.500-11: Methodology for subjective assessment of the quality of television pictures, 2002. [9](#)
- [War04] WARE C.: *Information Visualization: Perception for Design*. Morgan Kaufmann Publishers Inc., San Francisco, CA, USA, 2004. [7](#)
- [WRS*12] WU H.-Y., RUBINSTEIN M., SHIH E., GUTTAG J., DURAND F., FREEMAN W.: Eulerian Video Magnification for Revealing Subtle Changes in the World. *ACM Trans. Graph.* **31**, 4 (July 2012), 65:1–65:8. [3](#)
- [WWS03] WOODRING J., WANG C., SHEN H.-W.: High dimensional direct rendering of time-varying volumetric data. In *Visualization, 2003. VIS 2003. IEEE* (Oct 2003), pp. 417–424. [1](#), [3](#)

- [WYM08] WANG C., YU H., MA K. L.: Importance-Driven Time-Varying Data Visualization. *IEEE Trans. Vis. Comput. Graphics* 14, 6 (Nov 2008), 1547–1554. [1](#), [3](#)
- [YSL*14] YAN F., SHARF A., LIN W., HUANG H., CHEN B.: Proactive 3D Scanning of Inaccessible Parts. *ACM Transaction on Graphics* 33, 4 (July 2014), 1–8. [1](#)